STRENGTHENING MECHANISM OF $Ni_{53}Mo_{35}Fe_9B_2$ ALLOY

N.L. Perez
Department of Mechanical Engineering
University of Puerto Rico
Mayaguez, P.R. 00680, USA

ABSTRACT
The Cottrell and Orowan strengthening theories were merged for developing a linear analytical model of the Hall-Petch type relation that supports the observed precipitation hardening mechanism of a Ni-base alloy. The strengthening of the alloy was attributed to a fine dispersion of boride particles embedded in a strain hardened Ni/Mo-base metallic matrix. It was observed that this alloy exhibited excellent thermal stability due to the stable boride particles.

INTRODUCTION
It is well known [1-3] that rapidly solidified alloys (RSA's) exhibit thermodynamic stability, fine microstructures, and excellent mechanical, physical and magnetic properties. Some RSA's contain a uniform dispersion of particle, which is to a great extended the main source of enhanced mechanical properties. Unfortunately, RSA's are difficult to produce in bulk, although consolidation methods has shown promise of producing RSA's with unique microstructures and enhanced properties [1-6]. However, the superior properties of RSA's are degraded during hot consolidation, although it is possible to obtain a fine grained microstructure or a fine dispersion of particles for pinning grain boundaries. These particles (intermetallic phases) are very stable at relatively high temperatures and are embedded into the solid solution matrix, which strain hardens to induce appreciable ductility [7-12]. Hence, particle dispersion is an excellent source of strengthening of Ni-Mo-X-B alloy systems, in which X= Fe, Cr, Co or a combination of these. Detailed understanding of the precipitation hardening mechanisms requires particular consideration. For instance, the Hall-Petch relationship [13-14] and the Orowan strengthening mechanism (Orowan's theory) [15] are normally used to explain the strengthening of alloys that exhibit grain growth and a significant volume fraction of particles, respectively. Also, the Cottrell dispersion mechanism (Cottrell theory) [16] seems to be very attractive. However, during prolonged heat treatment, additional solid state processes are expected to take place, such as migration of vacancies or recrystallization of the matrix, which cause matrix softening.

The objective of this paper is to evaluate the strengthening mechanism of a RSA Ni-base alloy containing a uniform dispersion of precipitated boride particles. The theoretical evaluation of the strengthening mechanism is compared to the experimental results. In this account, the Cottrell and Orowan theories are used as the theoretical background in order to derive a Hall-Petch type equation.

FORMULATION

The theories of strengthening due to uniform dispersion of particles are thoroughly explained in Orowan and Cottrell [15-16]. In this section, only a brief summary of proposed analytical closed form expressions is given for calculating the parameters of the Hall-Petch type equation. The proposed expressions are based on the Cotter's and Orowan's strengthening theories with the aid of the model for dislocation pile up schematically shown in Figure 1.

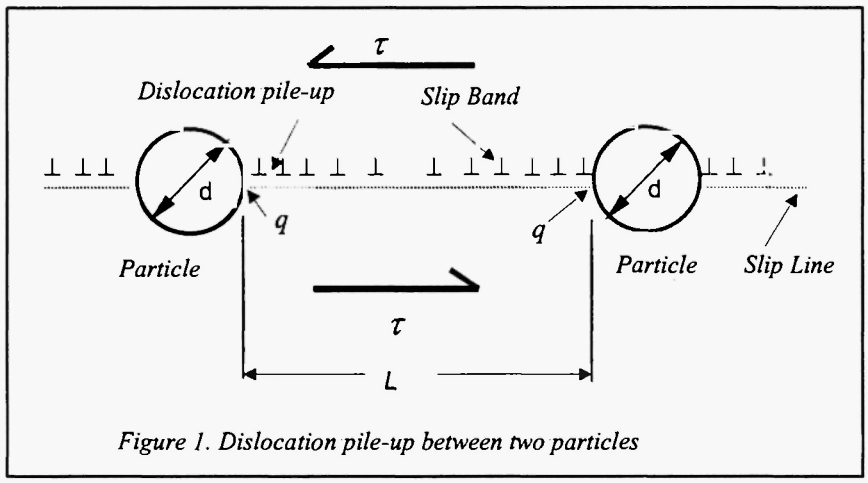

Figure 1. Dislocation pile-up between two particles

Assume that the particles exhibit a large volume fraction associated with a small mean free path, the particles are nearly spherical and that dislocation pile-ups are created between particles under the influence of an applied stress. The model for piling of dislocations ($\perp$) assumes that the dislocation source is located among obstacles (Figure 1) and a series of identical dislocations on a slip plane. The dislocation pile-up against obstacles causing an increase in the stress concentration at the particle-matrix interface. At equilibrium, the work done by N dislocations against the obstacles is [16]

$$W = N\sigma b\partial x \tag{1}$$

where σ = applied stress, b = Burgers vector, and ∂x = distance traveled by a dislocation.

It is also assumed, as per Figure 1, that the distance among dislocations decreases as they approach an obstacle, and that all dislocation move the same distance ∂x [16].

Merging Cottrell and Orowan strengthening (for non-shearing particles) theories develops the proposed expressions. That is,

The shear stress at the dislocation-particle interface is the Orowan stress for non-shearing particle [15]. Hence,

$$\tau_a = \alpha Gb / L \tag{2}$$

where $\alpha = d / L$ *=aspect ratio, G = shear modulus, b = Burger vector, L = edge-to-edge particle spacing, and d = particle size (diameter).*

According to the model depicted in Figure 1, the internal friction stress is

$$\sigma_o = 2\tau_o = 2\alpha Gb / L = 2Gbd / L^2 \tag{3}$$

The fracture stress for particles is [16]

$$\tau_p = q\tau_a \tag{4}$$

where $q = (b/d)^{1/2}$ *= stress concentration factor, and* τ_a *=applied shear stress.*

The number of dislocations that can be packed in a slip band of length L is [15]

$$N = \frac{4L\tau_a\kappa}{Gb} \tag{5}$$

where for screw dislocations $\kappa = 1$, *for edge dislocations* $\kappa = 1 - \nu$, ν *= Poisson's ratio. The shear stress for N dislocations along the slip band takes the form*

$$\tau = \frac{q\tau_a L}{Nb} \tag{6}$$

Using the definition of the maximum shear stress on a slip plane at 45° to the slip plane, $\sigma_p = 2\tau$, *and eq. (5) into eq. (6), it yields the particle stress*

$$\sigma_p = \left[\frac{0.5Gb^{1/2}}{\kappa}\right] d_p^{-1/2} = K_p d_p^{-1/2} \tag{7}$$

The term in brackets reflects the dislocation locking term (K_p), *and* σ_p *is the particle resistance stress, which is analogous to the grain boundary stress.*

Now, adding eqs. (3) and (7) can derive an expression of the Hall-Petch type for predicting the yield strength of a material containing a dispersion of hard (non-shearing) particles as the source of strengthening. Hence,

$$\sigma_{ys} = 2Gbd / L + \left[\frac{0.5Gb^{1/2}}{\kappa}\right] d_p^{-1/2} \tag{8}$$

or

$$\sigma_{ys} = \sigma_{op} + \sigma_p = \sigma_{op} + K_p d_p^{-1/2} \tag{9}$$

If $\kappa = 1$ in eq. (8), then $K_p = 0.5Gb^{1/2}$, which is the similar to Friedel equation [17], $K_p = 0.2Gb^{1/2}$, for the dislocation locking term for brittle materials.

Using $G = E/[2(1+\nu)]$ and $b = a/\sqrt{2}$ in eq. (8), it yields a more convenient equation

$$\sigma_{ys} = \frac{Ead}{\sqrt{2}(1+\nu)L^2} + \left[\frac{4Ea^{1/2}}{19(1+\nu)\kappa}\right] d_p^{-1/2} \tag{10}$$

Notice that the first term in eq. (10) depends on the particle size, and the second in brackets is a constant (slope). Hence,

$$\sigma_{op} = \frac{Ead}{\sqrt{2}(1+\nu)L^2} = f(d, L) \tag{11}$$

$$K_p = \left[\frac{4Ea^{1/2}}{19(1+\nu)\kappa}\right] = cons\tan t \tag{12}$$

where G = shear modulus (MPa), $b = a/\sqrt{2}$ = Burgers vector (m), a = lattice parameter of a FCC structure (m), L = particle spacing (edge-to-edge) (m), $q = d/L$ = stress concentration factor at the end of a dislocation pile-up and d = particle size (m), and σ_p = particle strength (MPa).

Equations (8) through (12) are the proposed expressions to be used for explaining the experimental results on precipitation hardening of the Ni-base alloy in question. For comparative purposes, the empirical Hall-Petch relation [13-14] for the yield strength of materials that exhibit grain growth is

$$\sigma_{ys} = \sigma_{oy} + K_y d^{-1/2} \tag{13}$$

and the Petch equation [14] for fracture strength is

$$\sigma_f = \sigma_{of} + K_f d^{-1/2} \tag{14}$$

where d is the grain size, σ_{ov} = friction stress for yielding, σ_{of} = intrinsic friction stress for fracture, K_y = = dislocation locking term, K_f = proportionality constant.

Moreover, eqs. (9) and (10) can be used for evaluating the strength of a dispersion-hardened alloy. The theoretical foundation of the proposed analytical expressions for yielding lies in the Cottrell [16] and Orowan [15] theories of dispersion hardening. However, the expressions for the fracture strength are purely empirical.

EXPERIMENTAL PROCEDURE

The material used in this investigation was a rapidly solidified alloy (RSA) type $Ni_{53}Mo_{35}Fe_9B_2$ (Devitrium 7025), which has been described elsewhere [7]. Monotonic tensile test and quantitative Metallography followed a heat treatment procedure at 1100 °C for 0, 24, 48 and 240 h, and air-cooled. Hounsfield No. 11 specimens were used to conduct the tension tests using a universal testing machine at a strain rate of 1.65×10^{-3} 1/s. The yield strength of the alloy was determined using the 0.2 % offset method. Microscopy studies included optical microscopy (OM), scanning electron microscopy (SEM), transmission electron microscopy (TEM), and X-ray diffraction. Specimens were electrolytically etched with Marble's reagent.

RESULTS AND DISCUSSION

Figure 2 shows the quantitative metallographic results. It is very interesting to note that the edge-to-edge particle spacing (L) increased very slightly; but the volume fraction (V_f) and particles size (d) increased significantly with increments of precipitation heat treatment time. Particle coarsening is evident in Figure 2, but the size of these particles is extremely small and their volume fraction is considerably large. These experimental results indicate that particle size in the range shown in Figure 2 are effective in promoting precipitation hardening. The basis of this explanation is that the extent to which dislocation moves is restricted to the small particle-to-particle distance and hard particles, enhancing the piling of dislocations against particles.

Moreover, nucleation and growth of fine boride particles occurred as a consequence of extrusion and heat treatment at 1100 °C. However, grains were difficult to reveal, but it was observed that this alloy contained a low dislocation density, which was insignificant for conducting quantitative work (Figure 3).

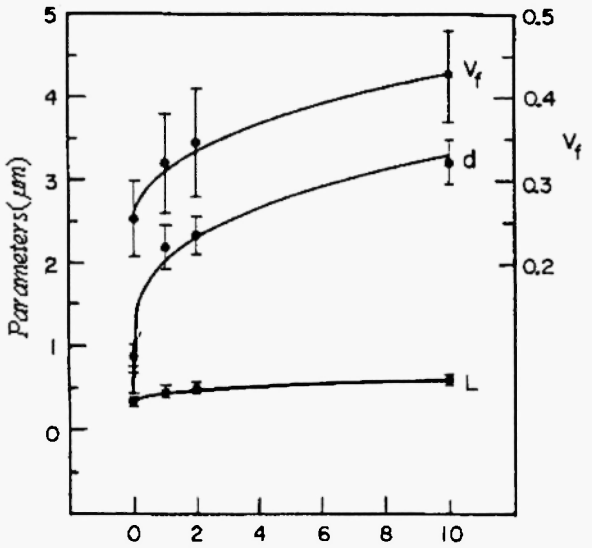

Figure 2. *Influence of heat treatment time on microstructural parameter of* $Ni_{53}Mo_{35}Fe_9B_2$.

Figure 3a illustrates the distribution, morphology and coarsening of the precipitated boride particles. Figure 3 elucidates some of the features that contributed to the data alluded to in Figure 2. This implies that precipitation heat treatment has an effect on the amount and size of precipitates, and thus the strength of the alloy. Transmission electron microscopy (TEM) was employed on strained to failure tensile specimens. It was revealed that all substructures were very clean and contained very low dislocation density, which was insufficient to quantify. Therefore, quantitative microscopy on TEM photomicrographs was not representative enough for developing correlations with mechanical properties. The mechanical strengthening of $Ni_{53}Mo_{35}Fe_9B_2$ alloy appears to be due to the dispersed particles. The classical Frank-Read dislocation loops were not observed. Therefore, it is apparent from Figure 3c and 3d that dislocations arise mainly from the particle-matrix interfaces. This further supports the precipitation hardening from the solid state at high temperatures.

Briefly, X-ray diffraction on extruded and heat-treated microstructures revealed the following boride phases Mo_2NiB_2 (orthorhombic) [5,11], Mo_2FeB_2 (tetragonal), and BFe_2 (tetragonal) for the extruded microstructure [11]. Also, Mo_2NiB_2, $MoFe_2B_4$ (orthorhombic), Mo_2FeB_2 (tetragonal) and BFe_3 (tetragonal) and $Fe_{23}B_6$ (cubic) for the microstructure heat treated at 1000 °C for 24 h [11].

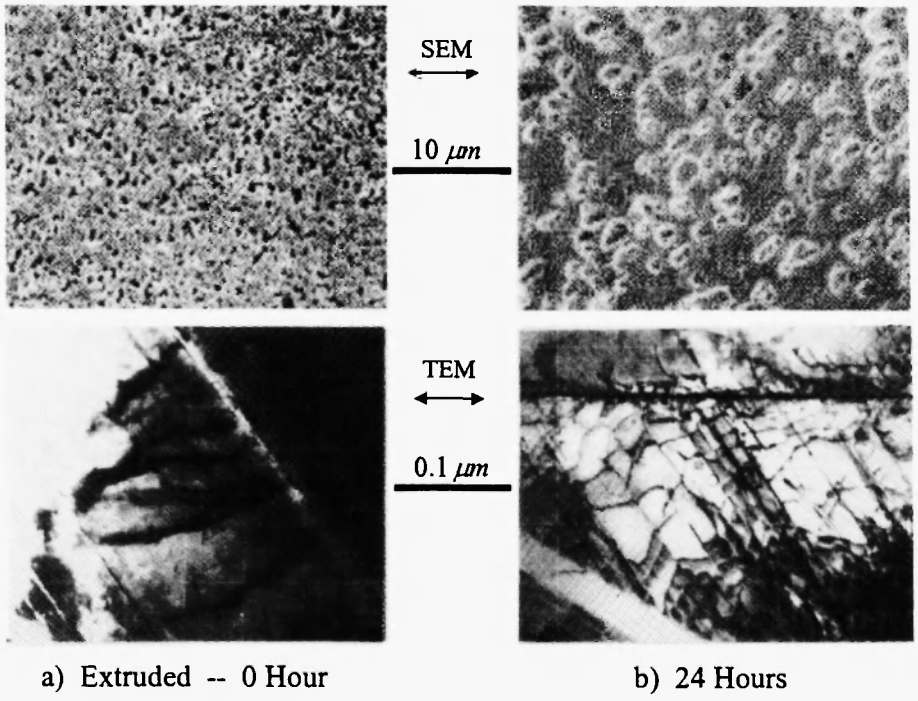

Figure 3. *SEM and TEM photomicrographs of showing the distribution, morphology and coarsening of dispersed boride, and dislocation network, respectively.*

It should pointed out that tensile stress-strain curves (not included herein) indicated that the alloy fractured at the maximum tensile stress. This implies that the alloy could not withstand a triaxial state of stresses. Therefore, all fractured tensile specimens broke perpendicularly to the tensile force direction, which is an indicative of brittle fracture mode. However, fractographic work revealed small dimples, indicative of ductile fracture mode (Figure 4). This corroborates the measured 20% elongation due to matrix strain hardening.

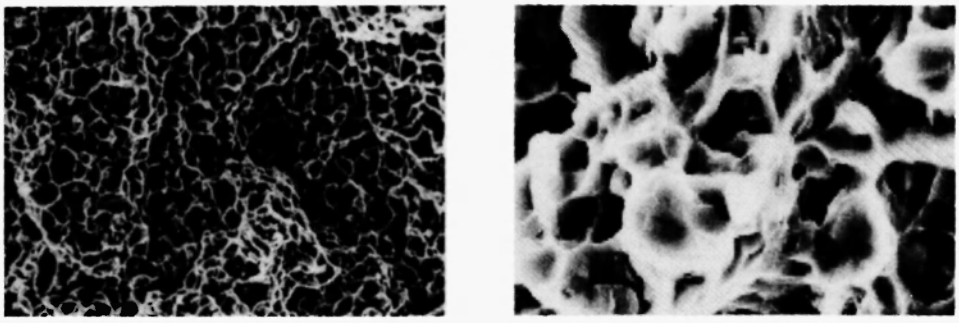

Extruded -- 0 Hours *Heat Treated for 24 Hours*

Figure 4. Fracture surfaces of tensile specimens showing small dimple size.

Figure 5 shows relationships between particle size and mechanical properties. These results indicate the usefulness of the eq. (9) for explaining the strengthening mechanism due to a dispersion of boride particles embedded in a strain hardened Ni-solid solution matrix. The Rockwell hardness was included as an additional information. It can be observed from Figure 6 that this alloy shows a slight decline in strength and hardness upon heat treatment at 1100 °C for 10 days. That is, the differences in strength and hardness between the extruded and the heat-treated microstructures are a) $\Delta\sigma_{ys} = 394\,MPa, \Delta\sigma_f = 329\,MPa,$ and b) $\Delta R_c = 11$ points.

On the other hand, total elongation (20%) and reduction in area (< 4%) remained basically unchanged. Surprisingly, these results indicate that this alloy is very stable at high temperatures. These observations agree with previous studies on Ni-Mo-X-B alloy systems [1-2]. Precipitation and coarsening of hard and brittle boride particles are attributed to contribute, to an extent, to the stability associated with enhanced homogeneity induced by rapid solidification processing (RSP). Despite the high strength of this alloy, it exhibits significant elongation, which is attributed to the relatively soft Ni-solid solution matrix. However, the reduction in area of < 4% may be attributed to the alloy not being able to withstand triaxial stresses at the onset of necking.

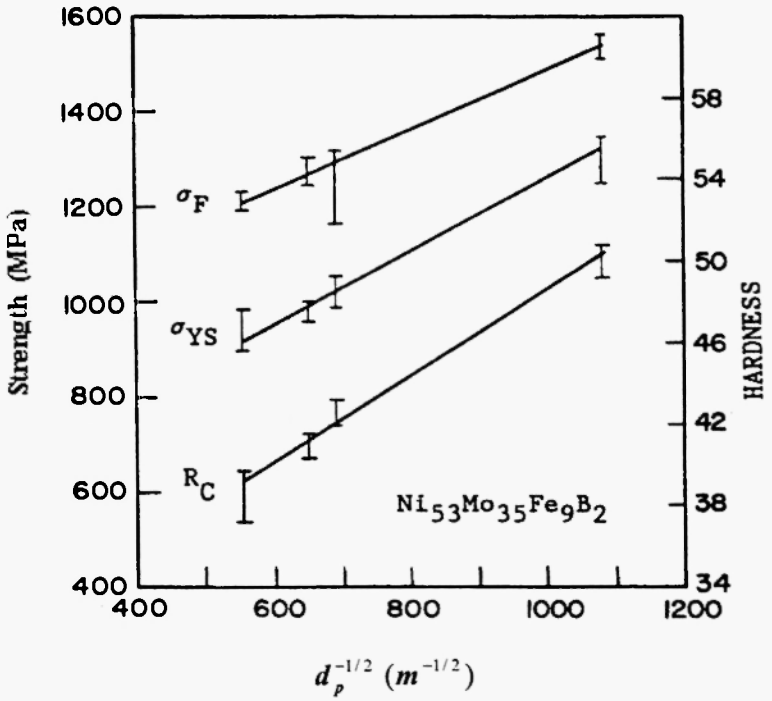

Figure 5. *T he Hall-Petch type relationship on the strength, Rockwell hardness.*

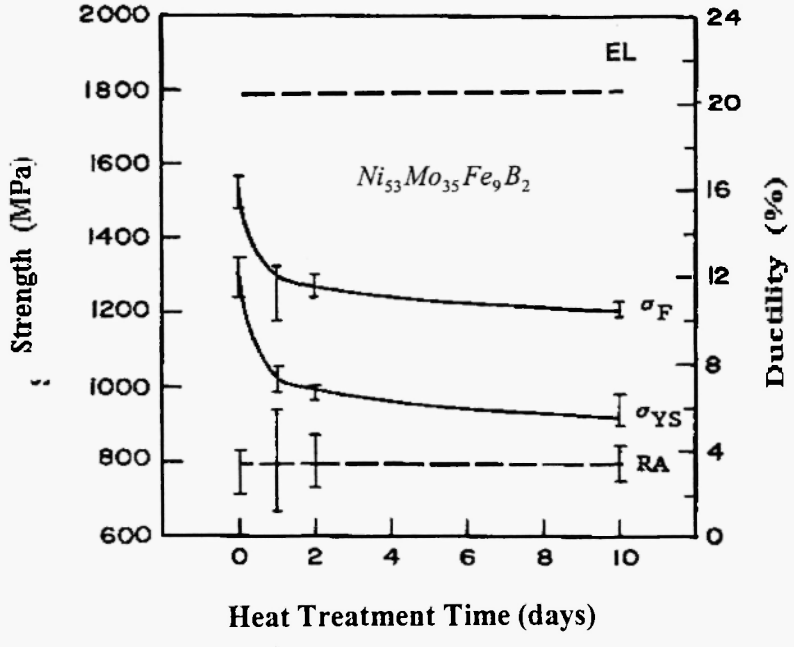

Figure 6. *Mechanical properties vs. annealing time at 1100 °C.*

Returning to the analytical expressions, it is of significant interest to determine the trend of σ_{op} as a function of heat treatment (HT) time. Figure 7 shows how this parameter changes with increasing HT time. In the present context, it should be noted that the decrease in σ_{op} with increasing HT time could be attributed to the solid state reactions of solute and the distribution of precipitated particles on dislocation motion [18-19]. In addition, σ_{op} is temperature-dependent and arises from the crystal lattice, making σ_{ys} a temperature-dependent property due to σ_{op} [22]. The striking observation is that σ_{op} in eq. (11) decreases with heat treatment time can be valid because σ_{op} is the matrix friction stress that opposes dislocation motion, and the less dislocations present in the matrix the lower the friction stress. Moreover, at prolonged heat treatment time, the migration of vacancies and recrystallization of the matrix may be attributed to contribute to the observed softening due to a decline in the intensity of internal stress; which reduce mechanical properties [23]. This may partially explain the data in Figure 7, which indicates that toughness, increases with precipitation heat treatment time due to a softening process of the microstructure. This indirectly supports the data shown in Figure 6; otherwise softening would not be possible.

When plastic flow occurs, an applied stress exceeds σ_{op} causing dissipation of surface energy per unit length as dislocations move a distance ∂x [21]. This concept supports the data shown in Figure 7 for σ_{op} being dependent on heat treatment time. Hence, the surface energy (γ_d) for dislocation motion is given by [21]

$$\gamma_d = \sigma_{op} b \partial x \tag{15}$$

For instance, the results shown in Figure 7 indicates that σ_{op} decreases with increasing heat treatment time t. This, then, implies that if the particle size is d_1 at time t_1, eq. (15) becomes $\gamma_{d_1} = \sigma_{op_1} b \partial x_1$ when dislocations move a distance ∂x_1. If $t_2 > t_1$, then $d_{p2} > d_{p1}$ and $\gamma_{d_2} = \sigma_{op_2} b \partial x_2$ since $\partial x_2 > \partial x_1$. This means that dislocations can move with less difficulty a distance ∂x_2. Therefore,

$$\sigma_{op_1} > \sigma_{op_2} \tag{16}$$

In general,

$$\sigma_{op_i} > \sigma_{op_{i+1}} \tag{17}$$

when $t_i < t_{i+1}$, $d_i < d_{i+1}$ and $\partial x_i < \partial x_{i+1}$, where i = 1, 2, 3 ....

In summary, since $Ni_{53}Mo_{35}Fe_9B_2$ was hot extruded, its initial high strength may be attributed, to a large extend, to the dispersion of boride particles; but the appreciable elongation is due to strain hardening of the matrix. In addition, curve fitting on the

experimental data gave the following equations

$$\sigma_{ys} = 491.23\ MPa + \left(0.7660\ MPa/\sqrt{m}\right)\cdot d_p^{-1/2} \qquad (r^2 = 0.99) \tag{18}$$

$$\sigma_f = 856.91\ MPa + \left(0.6270\ MPa/\sqrt{m}\right)\cdot d_p^{-1/2} \qquad (r^2 = 0.99) \tag{19}$$

$$R_c = 27.46 + 0.021\cdot d_p^{-1/2} \qquad (r^2 = 0.98) \tag{20}$$

In addition, a Ni-solid solution has a lattice parameter $a = 0.352\ nm$, and Burgers vector $b = a/\sqrt{2} = 0.2492\ nm$. The alloy used to generate the experimental data has the following properties [2]: Modulus of elasticity $E = 217{,}241.38\ MPa$ $(30.5x10^6\ MPa)$, and Poisson's ratio $\nu = 0.22$. Then, the shear modulus is $G = E/[2(1+\nu)] = 89{,}033\ MPa$ and the dislocation locking term, as per eq. (12) with $\kappa = 1$, is

$$K_p = \left[\frac{4Ea^{1/2}}{19(1+\nu)\kappa}\right] = 0.7033\ MPa\sqrt{m} \qquad \textbf{(Theoretical)} \tag{21}$$

$$K_p = 0.766\ MPa\sqrt{m} \qquad \textbf{(Experimental)} \tag{22}$$

Notice that the proposed analytical procedure is in good agreement with the experimental data since there is approximately 8% error between the theoretical and experimental values for K_p.

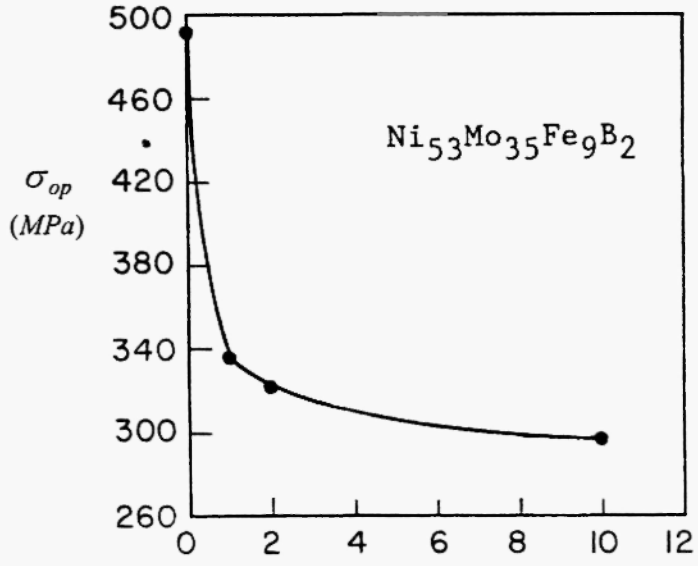

Figure 7. *Influence of HT time (days on the friction stress.*

CONCLUSIONS

This alloy showed excellent thermal stability due to a microstructural stability which was attributed to boride particles, specially the two more stable boride phases, Mo_2NiB_2 and Mo_2FeB_2 [7,11]. High strength and high hardness were evident, but ductility was appreciable at 20% elongation. However, a reduction in area of < 4% was apparently related to the onset of particle fracture when triaxial stresses were present and to particle-matrix separation. The strengthening mechanism was mainly attributed to the uniform dispersion of boride particles since the alloy showed very low dislocation density. This was explained using a proposed analytical model based on Cottrell and Orowan strengthening theories, which led to the Hall-Petch type equation. It was shown that the friction stress σ_{op} and the dislocations locking term K_p for yielding is in good agreement with the curve-fitting result, eq. (22).

REFERENCES

1. Raybould, D., Carbide Tool Journal, (November-December 1984) 26-27
2. Raybould, D., Power Metallurgy Report, 39 (5) (1984)
3. Das, S.K. and Raybould, D., in Proc. of the Fifth Conference on Rapid Quenching and Solidification of Metals (RQ5), Wurzberg, reprint, (3-7 September) 1984).
4. Das, S.K et al., in Proceedings of the Third Conference on Rapid Solidification Processing, Gaithersburg, Maryland, USA, reprint, (6-8 December 1982).
5. Das, S.K., Okasaki, K, and Adam, C.M., in Proc. Conference on High Temperature Alloys: Theory and Design, Bethesda, Maryland, USA, reprint, (9-11 April 1984)
6. Wan, C.C., in Proceedings of the Materials Research Society Annual Meeting, edited by B.H. Kear, B.C. Giessen and M. Cohen, (November 1982) 441.
7. Perez, N.L., Ph.D. thesis, University of Idaho, Moscow, Idaho, USA, (1989)
8. Perez, N.L., Place, T.A., and Bobeck, G.E., Slip Lines **14(4)**, (December 1987) 6.
9. Place, T.A., Perez, N.L., G.E. Bobeck, G.E., P.R. Mantena and Gibson, R.F., in Proceedings of Advanced Materials Symposium, ISTFA/87, International Society Testing and Failure Analysis, ASM international, Metals Park, Ohio, USA, (November 9-13, 1987) 103-108.
10. B.G. Giessen, B.G., Polk D.E., and RAY, R., in High Strength Iron, Nickel and Cobalt Base Crystalline Alloys with Ultrafine Dispersion of Borides and Carbides, USA, Patent 4,297,137; (October 1981).
11. Perez, N.L., and Place, T.A., Journal of Materials Sci. Letters, 9(1990) 940-942.
12. Taub, A.I., and Jackson, M.R., in Rapidly Solidified Alloys and Their Mechanical and Magnetic Properties, Materials Research Society Symposium Proceedings, edited by B.C. Giessen, D.E. Polk and A. I. Taub, **58** (1986) 398.
13. Hall, E.O., in Proceedings of the Royal Society of London, B64 (1951) 474.
14 Petch, N.J., Journal of Iron and Steel Institute of London, **174** (1953) 192.
15. Orowan, E., discussion in Symposium on Internal Stresses, Institute of Metals, London (1947) 451.

16. Cottrell, A.H., "Dispersion and Plastic Flow in Crystals," The inter Series of Monographs on Physics, Oxford, Clarendon Press, (1953) 104-107.
17. Friedel, J., "Dislocations," Pergamon Press, Addison-Wesley publishing company, Reading, Massachusetts, (1964) 268.
18. Nicholson, R.B., "strengthening Methods in Polycrystals," edited by Kelly and R.B. Nicholson, Halsted Press division, John Wiley & Sons, New York, (1971) 537-539.
19. Wilson, D.V., Mat. Sci. J., (1967) 40.
20. Armstrong, R.W., "Grain Size: The Fabric of (Brittle) Fracture of Polycrystals", Fracture 1977, Vol. 4, ICF4, Waterloo, Canada, (June 19-24, 1977) 61-74.
21. L.M. Brown, L.M., and Ham, R.K., "strengthening Methods in Polycrystals", edited by A. Kelly and R.B. Nicholson, Halsted Press Division, John Wiley and Sons, Inc., New York, (1971) 14, 34, 39,92.
22. N.J. Petch and R.W. Armstrong, Acta Metall. Vol 37 No. * (1989) 2279.
23. A.H. Cottrell, "Dislocation and Plastic Flow in Crystals," Oxford University Press, Amen House, London E.C.4 (1958) 133

ACKNOWLEDGEMENT

This work was supported by the Interior Department's Bureau of Mines under contract No. J01340035. Special thanks go to Dr. T.A. Place and G. Bobeck for their support.